LJMU Research Online

Kamaris, GS, Skalomenos, KA, Hatzigeorgiou, GD and Beskos, DE

 Seismic damage estimation of in-plane regular steel/concrete composite moment resisting frames

http://researchonline.ljmu.ac.uk/id/eprint/3755/

Article

For more information please contact researchonline@ljmu.ac.uk

Seismic damage estimation of in-plane regular steel/concrete composite moment resisting frames

George S. Kamaris[1], Konstantinos A. Skalomenos[2], George D. Hatzigeorgiou[3,*] and Dimitri E. Beskos[4,5]

[1] School of Engineering, University of Warwick, Coventry CV4 7AL, United Kingdom

[2] Disaster Prevention Research Institute (DPRI), Kyoto University, Gokasho, Uji, Kyoto 611-0011, Japan

[3] School of Science and Technology, Hellenic Open University, GR-26335 Patras, Greece

[4] Department of Civil Engineering, University of Patras, GR-26500 Patras, Greece

[5] Office of Theoretical and Applied Mechanics, Academy of Athens, 4 Soranou Efessiou, GR-11527 Athens, Greece.

Abstract: Simple empirical expressions to estimate maximum seismic damage on the basis of four well known damage indices for planar regular steel/concrete composite moment resisting frames having steel I beams and concrete filled steel tube (CFT) columns are presented. These expressions are based on the results of an extensive parametric study concerning the inelastic response of a large number of frames to a large number of ordinary far-field type ground motions. Thousands of nonlinear dynamic analyses are performed by scaling the seismic records to different intensities in order to drive the structures to different levels of inelastic deformation. The statistical analysis of the created response databank indicates that the number of stories, beam strength ratio, material strength and ground motion characteristics strongly influence structural damage. Nonlinear regression analysis is employed in order to derive simple formulae, which reflect the influence of the aforementioned parameters and offer a direct estimation of the damage indices used in this study. More specifically, given the characteristics of the structure and the ground motion, one can calculate the maximum damage observed in column bases and beams. Finally, three examples serve to illustrate the use of the proposed expressions and demonstrate their accuracy and efficiency.

Keywords: Steel/concrete composite frames; Moment resisting frames; Damage indices; Seismic assessment; Ordinary ground motions.

---

* Corresponding author: Tel.:+30.2610.367769
  E-mail address: hatzigeorgiou@eap.gr

1. Introduction

Damage in a structure under loading can be defined as the degradation or deterioration of its integrity resulting in reduction of its load capacity. In earthquake-resistant design of structures, some degree of damage in the structural members is generally accepted. This is done because the cost of a structure designed to remain elastic during a severe earthquake would be very large. Thus, existing seismic codes, e.g., EC8 [1], in an implicit way and more recent performance-based seismic design methods [2-4] in an explicit and more systematic way employ the concept of damage to establish structural performance levels corresponding to increasing levels of earthquake actions. These performance levels mainly describe the damage of a structure through damage indices, such as the inter-story drift ratio (IDR), or the member plastic rotations.

Several methods to determine damage indices as functions of certain response parameters have been presented in the literature. In general, these methods can be noncumulative or cumulative in nature. The most commonly used parameter of the first class is ductility, which relates damage only to the maximum deformation and is still regarded as a critical design parameter by codes. To account for the effects of cyclic loading, simple rules of stiffness and strength degradation have been included in various noncumulative indices [5-7], mainly referred to reinforced concrete members. Cumulative-type indices can be divided in deformation based [8] or hysteresis based [9,10] formulations and methods that consider the effective distribution of inelastic cycles and generalize the linear law of low-cycle fatigue of metals through a hypothesis of linear damage accumulation [11]. Sucuoğlu and Erberik [12] developed low-cycle fatigue damage models for deteriorating systems on the basis of test data and analysis and Kamaris et al. [13] proposed a new damage model exhibiting strength and stiffness degradation which takes into account the phenomenon of low-cycle fatigue and the interaction between axial force and bending moment at a section of a beam-column steel member. Combinations of deformation and energy dissipation have been also proposed to establish damage indices [14]. In these methods damage is expressed as a linear combination of the damage caused by excessive deformation and that due to repeated cyclic loading effects [14]. An extensive review of damage indices used in the literature can be found in Powell and Allahabadi [15]. Finally, the concept of continuum damage mechanics [16] in conjunction with the finite element method of concentrated inelasticity has been employed in the analysis of steel and reinforced concrete structures [17,18] for the determination of their damage.

The composite moment resisting frames (MRFs) having concrete-filled steel tube (CFT) columns and steel girders (CFT-MRFs) (Fig. 1) are a relatively new type of structures which offers significant advantages for use as the primary resistance systems in building structures subjected to seismic loading. The CFT-MRF systems exhibit desirable features, such as large energy dissipation

and increased strength and stiffness to control the drifts. For these reasons, they have increasingly investigated during the last decades for understanding their behaviour under seismic loads [19-21] and have been popular in mid-rise and high-rise buildings in Japan and the U.S.
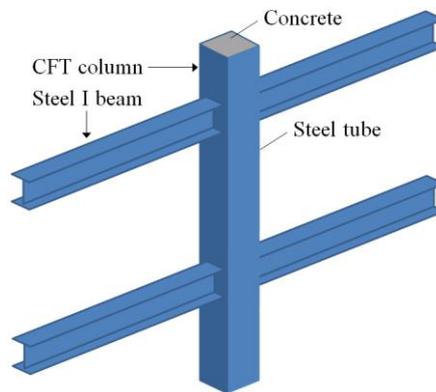

Fig. 1. CFT-MRF configuration

The main objective of this paper is to study the seismic inelastic behaviour of CFT-MRFs and quantify their damage through simple expressions that relate the most commonly used damage indices of the literature with the characteristics of the frames and the ground motions. Similar expressions have been proposed by the authors for steel MRFs and x-braced frames [22], but research on CFT-MRFs is still missing. For that reason, a large number of CFT-MRFs are subjected to an ensemble of 100 ordinary (i.e. without near-fault effects) ground motions scaled to different intensities. A response databank is created and a regression analysis is performed in order to derive simple formulae that can be used for the prediction of damage. Two examples are utilized to illustrate the use of the proposed formulae and demonstrate their efficiency and accuracy. It should be pointed out that the seismic damage calculated herein is "probably expected" and not a deterministic damage value, since the procedures utilized in this paper are based on statistical formulae.

The proposed methodology provides the means of a rapid and accurate damage assessment of existing structures, avoiding the use of the more sophisticated and time consuming non-linear dynamic analysis. It can also be utilized in the preliminary design of structures in the framework of a performance based design approach in order to size a frame to achieve a preselected damage level. Thus, the designer can perform a high quality preliminary design based on elastic analysis and the proposed relationships, which can significantly decrease the need for iterations in an analysis/design procedure. This is very important when analysis is non-linear dynamic and time consuming. Finally, the main advantages of the proposed formulae are simplicity, accuracy and rapid damage estimation, which is usually done by advanced and costly methods of analysis.

2. Damage indices used in this study

The proposed damage expressions are associated with four damage indices existing in the literature. These are the damage indices of Park and Ang [14], Bracci et al. [10], Roufaiel and Meyer [6] and Banon and Veneziano [5]. These indices have been selected here because i) are the most widely used in applications and ii) can be easily employed with the aid of the Ruaumoko 2D program [23]. In the following, a brief description of all these four damage indices will be given for reasons of completeness.

The damage index D_{PA} of Park and Ang [14] is expressed as a linear combination of the damage caused by excessive deformation and that contributed by repeated cyclic loading effects, as shown in the following equation:

$$D_{PA} = \frac{\delta_m}{\delta_u} + \frac{\beta}{Q_y \delta_u} \int dE \qquad (1)$$

In the above, the first part of the index is expressed as the ratio of the maximum experienced deformation δ_m to the ultimate deformation δ_u under monotonic loading. The second part is defined as the ratio of the dissipated energy $\int dE$ to the term $(Q_y \, \delta_u)/\beta$, where Q_y is the yield strength and the coefficient β is a non-negative parameter determined from experimental calibration. In this work β is taken equal to 0.025 for the steel beams [24] and 0.03 for the CFT columns [25] of the frames used herein.

Bracci et al. [10] suggested a damage index equal to the ratio of 'damage consumption' (loss in damage capacity) to 'damage potential' (capacity), defined as appropriate areas under the monotonic and the low-cycle fatigue envelopes. Thus, the 'damage potential' D_P is defined as the total area between the monotonic load–deformation curve and the fatigue failure envelope. As damage proceeds, the load–deformation curve degrades, resulting in the damage D_s due to the loss of strength, while the irrecoverable deformation causes the deformation damage D_D. Thus, this damage index D_{BRM} is expressed as

$$D_{BRM} = \frac{D_D + D_S}{D_P} \qquad (2)$$

Roufaiel and Meyer [6] proposed that the ratio between the secant stiffness at the onset of failure M_m / ϕ_m and the minimum secant stiffness reached so far M_x / ϕ_x, can be used as a good

indicator of damage. Based on that, they defined the modified flexural damage ratio (MFDR) or D_{RM} as

$$D_{RM} = MFDR = \max[MFDR^+, MFDR^-] \tag{3}$$

$$MFDR^+ = \frac{\phi_x^+}{M_x^+} - \frac{\phi_y^+}{M_y^+} \left/ \frac{\phi_m^+}{M_m^+} - \frac{\phi_y^+}{M_y^+} \right. , \quad MFDR^- = \frac{\phi_x^-}{M_x^-} - \frac{\phi_y^-}{M_y^-} \left/ \frac{\phi_m^-}{M_m^-} - \frac{\phi_y^-}{M_y^-} \right. \tag{4}$$

where ϕ is the beam curvature due to a bending moment M, the term M_y/ϕ_y is the initial elastic stiffness and subscripts $+$ and $-$ denote the loading direction.

The Banon and Veneziano [5] analysis is set in a probabilistic context and their model has been calibrated on the basis of 29 different tests on reinforced concrete elements and structures, selected from among the most representative ones in the technical literature. In particular, the damage parameters d_1 and d_2 are defined, respectively, as the ratio of stiffness at yielding point to secant stiffness at failure, and the plastic dissipated energy E_h normalized with respect to the absorbed energy at the elastic limit. If the elastic-plastic model is used, d_1 is obviously equal to the ratio of the maximum displacement x_{max} to the displacement at the elastic limit x_y. Therefore, according to the notation introduced above, parameters d_1 and d_2 can be expressed as

$$d_1 = x_{\max}/x_y, \quad d_2 = E_h/(1/2)F_y x_y \tag{5}$$

where F_y is the yield strength. Furthermore, modified damage parameters d_1^* and d_2^* are introduced of the form

$$d_1^* = d_1 - 1 \tag{6}$$

$$d_2^* = a d_2^b \tag{7}$$

where a and b are two parameters which characterize the structural problem and are defined experimentally. For flexure, x and F are replaced by θ and M, respectively. Thus, the damage index D_{BV} is defined as

$$D_{BV} = \sqrt{(d_1^*)^2 + (d_2^*)^2} \tag{8}$$

3. Plane regularCFT-MRFs used in this study

3.1 Design and characteristics

A family of 48 plane regular (orthogonal without setbacks) along their height CFT-MRFs are designed for the parametric study of this work aiming to cover a wide range of structural characteristics of this type of composite structures. These frames have storey height and bay width equal to 3 m and 5 m, respectively, and CFT column sections, as shown in Fig. 2, with b and t being the side and thickness, respectively, of the square steel tubular cross-section of columns containing concrete. Moreover, the frames have the following structural characteristics: number of stories, n_s, with values 1, 3, 6, 9, 12, 15, 18 and 20, number of bays, $n_b = 3$, steel yielding stress ratio $e_s = 235 / f_s$ with the yielding stress f_s taking the values of 275 and 355 MPa, concrete strength ratio $e_c = 20 / f_c$ with the compressive strength f_c taking the values 20 MPa. Additionally, the beam-to-column stiffness ratio, ρ and column to beam strength ratio, α, taking various values within practical limits are also considered.
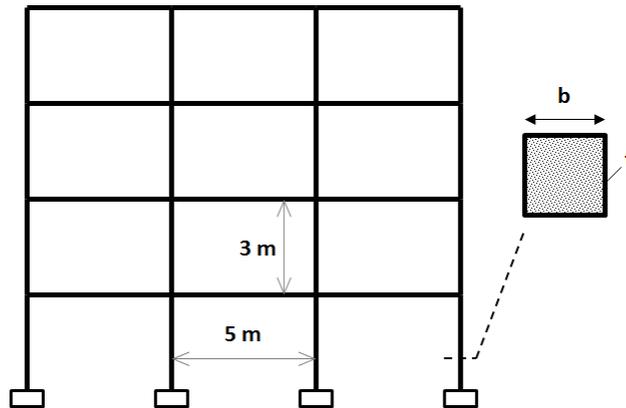
Fig. 2. Typical geometry of frames considered with columns of square concrete filled steel tube (CFT) sections.

The beam-to-column stiffness ratio ρ of a frame is based on the beam and column properties in the storey closest to the mid-height of the frame and calculated by

$$\rho = \frac{\sum (I/l)_b}{\sum (I/l)_c} \tag{9}$$

where I and l are the second moment of inertia and length of the steel member (column c or beam b), respectively. The concrete core is considered as cracked and the effective second moment of inertia for the composite section is defined according to EC4 [26]. Karavasilis et al. [27] have

6

introduced during the investigation of the inelastic seismic response of steel MRFs the beam strength ratio, *α,* which indicates how much stronger are the beams in comparison with the base columns. Following [27], the strength ratio, α, adopted here is defined as

$$\alpha = M_{RC,1,av} / M_{RB,av} \tag{10}$$

where $M_{RC,1,av}$ is the average of the plastic moments of resistance of the columns of the first storey (including the influence of axial load for gravity-earthquake loading combination) and $M_{RB,av}$ is the average of the plastic moments of resistance of the beams of all the stories of the frame. This parameter quantifies the structural capacity to avoid the formation of a global plastic mechanism which is developed when plastic hinges occur at the base of columns of the first floor and at the ends of beams.

The CFT-MRFs are designed according to the structural Eurocodes 3 [28], 4 [26] and 8 [1] with the aid of the computer programs SAP2000 [29] and MATLAB [30]. The parametric study of this work is not based on the design of a 3D prototype building but on 2D CFT-MRFs. The seismic load combination consists of the gravity load G + 0.3Q = 27.5 kN/m on beams plus the earthquake load and the gravity load combination 1.35G + 1.5·Q = 42.6 kN/m with G = 26 kN/m and Q = 5 kN/m being the dead and live floor loads, respectively. Columns are not subjected to biaxial flexure. The earthquake load is determined using design ground acceleration $\alpha_g = 0.30$g, soil type B (soil factor S = 1.2) and Spectrum Type 1 with behaviour factor q = 4. In addition to the satisfaction of the seismic strength demands in members, other seismic design checks include compliance with stability and drift criteria as well as capacity design considerations.

Data for 24 of the 48 frames considered here, including values for n_s, ρ, α, beam and column cross-sections and fundamental periods of vibration, are presented in Table 1, for 275 MPa yield steel stress. The sectional dimensions of the remaining 24 frames with 355 MPa yield steel stress are the same in order to clarify the effect of that material parameter. In this table, numeric forms, such as, 300×12.5 (1-4) and 300x10 (5-6), mean that the first four stories have CFT columns with square steel tubes of width b = 300 mm and thickness t = 12.5 mm, whereas the next two higher stories have CFT columns with square steel tubes of b = 300 mm and t = 10 mm, while numeric forms, such as, 400 (2-5), mean that stories from 2 to 5 have IPE 400 beams.

Table 1. Characteristics of CFT-MRFs considered in the study.

No.	n_s	ρ	α	T [s]	Columns [CFT] (floors)	Beams [IPE] (floors)
1	1	0.274	1.917	0.354	220x10 (1)	240 (1)
2	1	0.150	2.743	0.290	260x10 (1)	240 (1)
3	1	0.084	4.506	0.237	300x12.5 (1)	240 (1)
4	3	0.229	2.322	0.844	250x12.5 (1-3)	270 (1-3)
5	3	0.125	3.435	0.749	300x12.5(1-3)	270 (1-3)
6	3	0.082	4.489	0.690	340x12.5(1-3)	270 (1-3)
7	6	0.254	2.246	1.277	300x12.5 (1-4), 300x10 (5-6)	330 (1-4), 300 (5-6)
8	6	0.173	3.170	1.204	320x16 (1-4), 320x12.5 (5-6)	330 (1-4), 300 (5-6)
9	6	0.083	5.118	1.093	400x16 (1-4), 350x20 (5-6)	330 (1-4), 300 (5-6)
10	9	0.339	2.139	1.517	320x16 (1-5), 320x12.5 (6-7), 300x12.5 (8-9)	360 (1), 400 (2-5), 360 (6-7), 330 (8-9)
11	9	0.191	2.847	1.416	400x12.5 (1-5), 350x12.5 (6-7), 300x12.5 (8-9)	360 (1), 400 (2-5), 360 (6-7), 330 (8-9)
12	9	0.094	5.413	1.289	450x20 (1-5), 420x20 (6-7), 400x16 (8-9)	360 (1), 400 (2-5), 360 (6-7), 330 (8-9)
13	12	0.300	2.383	1.753	400x12.5 (1-5), 350x12.5 (6-8), 320x12.5 (9-10), 300x10 (11-12)	400 (1), 450 (2-5), 400 (6-8), 360 (9-10), 330 (11-12)
14	12	0.162	3.919	1.630	420x20 (1-5), 400x16 (6-8), 350x20 (9-10), 350x14 (11-12)	400 (1), 450 (2-5), 400 (6-8), 360 (9-10), 330 (11-12)
15	12	0.077	6.895	1.517	500x25 (1-5), 500x16 (6-8), 450x16 (9-10), 400x20 (11-12)	400 (1), 450 (2-5), 400 (6-8), 360 (9-10), 330 (11-12)
16	15	0.260	2.741	1.940	420x16 (1-5), 400x14 (6-8), 350x16 (9-11), 320x16 (12-13), 320x12.5 (14-15)	400 (1), 500 (2-5), 450 (6-8), 400 (9-11), 360 (12-13), 330 (14-15)
17	15	0.126	4.853	1.786	500x20 (1-5), 450x22.5 (6-8), 420x20 (9-11), 420x14 (12-13), 400x14 (14-15)	400 (1), 500 (2-5), 450 (6-8), 400 (9-11) 360 (12-13), 330 (14-15)
18	15	0.070	7.186	1.702	600x20 (1-5), 550x20 (6-8), 500x20 (9-10) 450x20 (11-12), 420x20 (14-15)	400 (1), 500 (2-5), 450 (6-8), 400 (9-11) 360 (12-13), 330 (14-15)
19	18	0.281	3.390	2.143	450x20 (1-5), 420x16 (6-9), 400x16 (10-13), 350x16 (14-16), 350x12.5 (17-18)	450 (1), 500 (2-9), 450(10-12) 400 (13-15), 360 (16-18)
20	18	0.192	4.280	2.055	500x20 (1-5), 450x20 (6-9), 420x20 (10-13), 420x12.5 (14-16), 350x16 (17-18)	450 (1), 500 (2-9), 450(10-12) 400 (13-15), 360 (16-18)
21	18	0.138	5.282	1.995	550x20 (1-5), 500x20 (6-9), 450x20 (10-13), 420x16 (14-16), 400x12.5 (17-18)	450 (1), 500 (2-9), 450(10-12) 400 (13-15), 360 (16-18)
22	20	0.287	3.338	2.390	450x20 (1-6), 420x16 (7-11), 400x16 (12-15), 350x16 (16-18), 320x16 (19-20)	450 (1-2), 500 (3-11), 450 (12-14), 400 (15-17), 360 (18-20)
23	20	0.181	4.214	2.284	500x20 (1-6), 450x22.5 (7-11), 420x20 (12-15), 400x16 (16-18), 350x20 (19-20)	450 (1-2), 500 (3-11), 450 (12-14), 400 (15-17), 360 (18-20)
24	20	0.101	6.300	2.162	600x20 (1-6), 550x20 (7-11), 500x20 (12-15), 450x20 (16-18), 420x20 (19-20)	450 (1-2), 500 (3-11), 450 (12-14), 400 (15-17), 360 (18-20)

3.2 Modelling for nonlinear analysis

The 48 CFT-MRFs mentioned in the previous section, are subject to a set of 100 accelerograms and their response to those motions is determined through inelastic dynamic time-history analysis using Newmark's constant average acceleration method with the aid of the computer analysis program Ruaumoko 2D [23]. Diaphragm action is assumed at every floor and the effect of large deformations is taken into account. Rayleigh type damping corresponding to 3% of the critical damping in the first and second mode is assumed. The deteriorating inelastic behaviour of all the frame members is modelled by means of zero-length plastic hinges. Finally, the effect of panel zones (PZs) was modelled by using the scissors model [31], assuming that the connections are rigid.

The Ramberg–Osgood hysteresis model is selected for simulating the seismic behaviour of steel beams. Degradation effects can be included in the Ramberg-Osgood model with the aid of the Ruaumoko's strength degradation model, which consists of a backbone curve based on ductility demands [23], as shown in Fig. 3. The strength reduction variation of Fig. 3 can be defined using the three parameters: DUCT1, which is the ductility at which the strength degradation begins, DUCT2, which is the ductility at the end of strength degradation, DUCT3, which is the ductility at 1% initial strength, and RDUCT, which is the ratio of the residual strength over the initial yield strength. The parameters which define the strength reduction variation of Ruaumoko's strength degradation model can be determined using the proposed relationships by Lignos and Krawinkler [33] in conjunction with the PEER/ATC 72-1 [34] guidelines. The modified Al-Bermani model developed by Skalomenos et al. [32] is used to simulate the hysteretic behaviour of CFT columns. This model is selected for two reasons: (i) the model was calibrated by Skalomenos et al. [32] for a wide range of values of the geometrical and strength parameters and (ii) the model is a simple concentrated plasticity model that can provide very good predictions of the force-deformation responses of CFT columns to cyclic loading, which exhibit material deterioration. Thus, the analytical models considered here account for nonlinearities due to yielding and local buckling of the steel beams and steel tubes of the CFT columns, cracking and crushing of concrete in the CFT columns and steel yielding and concrete cracking in the PZs. All the analytical models of frame components utilized here are based on concentrated plasticity theory and are presented in detail in Skalomenos et al. [32, 35], where the accuracy of the numerical response predictions is shown in a wide range of comparisons between numerical and experimental results. Finally, the modelling/analysis for the CFT columns take into account the bending moment – axial load (M – N) interaction diagram, such as the one described in Zhao et al. [36] according to Eurocode 4 [26].
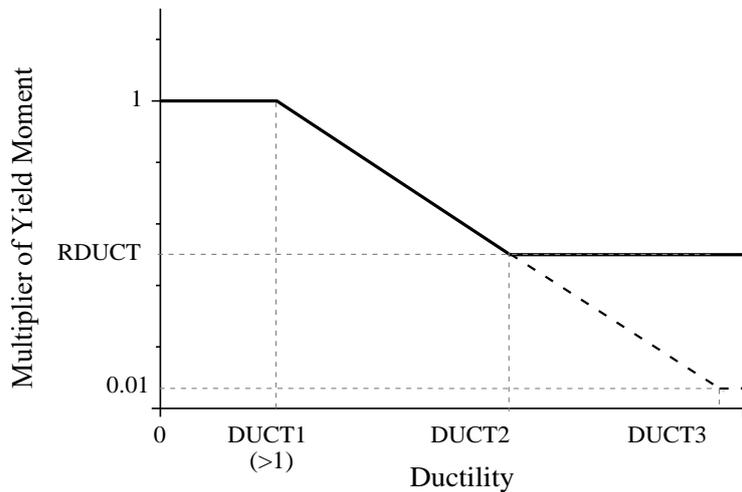
Fig. 3. Strength reduction variation using ductility terms [23].

3.3 Model validation

The composite MRF investigated experimentally by a pseudodynamic testing method by Herrera et al. [20] is used here to verify the validity of the aforementioned models for individual components (columns, beams, connections, and PZ) of a CFT-MRF by comparing its response to acceleration records at different seismic hazards as obtained experimentally and numerically with the aid of RUAUMOKO [23]. This frame is a 0.6-scale two-dimensional model of an external four-story/two-bay CFT-MRF of a three-dimensional prototype building, as shown in Fig. 4(a). In addition to the four stories above the ground, the frame also has a basement level and consists of rectangular CFT columns, wide flange beams, and split-tee moment connections. A typical interior joint of the frame and its analytical model are shown in Fig. 4(b) to illustrate the connectivity between the element models. The column model end nodes are at the boundary of the PZ, and the beam model end nodes are connected through the connection model to the nodes on the PZ boundary at the face of the column. The beam end nodes and PZ boundary nodes have the same horizontal displacement, and their vertical and rotational DOFs are connected by the vertical and rotational springs of the spring connection model, respectively.

In the analysis model, the P-Δ effects due to lateral displacements are taken into account through a leaning column with properties determined from the interior gravity frames of the prototype building. The leaning column is connected to the frame through loading beams attached to the midpoint of the steel girders at both bays of the structure with pin connections, as shown in Fig. 4(a). Additionally, the column is continuous, pinned at its base and constrained to have the same lateral displacement as the floor at each floor level. Consistent with the pseudodynamic model designed for the experiment, the loading beams are modelled as rigid links with large stiffness values. The section properties of the leaning column are calculated as the sum of the section

10

properties of one-half of the interior columns tributary to the prototype building. The mass of the structure is assumed to be lumped to the nodes of the leaning column at the story heights. Stiffness and mass proportional damping (Rayleigh damping) are assumed with proportionality factors of 0.1547 and 0.001194 for the stiffness and mass matrices, respectively, as a result of assumed 2% viscous damping in the first and third modes. The measured geometric and material properties of the structure members are utilized for determining the necessary parameters for the analytical models of individual components of the numerically analysed frame. It should be noted that the test structure has already been scaled down with the relevant multiplier factors by Herrera et al. [20]. As mentioned earlier, the experiment was conducted under different hazard levels. First, the frame was subjected to the Imperial Valley Array 04 (1979) ground motion record representing a frequently occurring earthquake (FOE). The accelerogram scale factor for the FOE level was 0.400. The maximum roof displacement was measured as 0.6% of the building height, and the structure remained primarily elastic. Second, the structure was loaded according to the Northridge Canoga Park (1994) ground motion record scaled to the design basis earthquake (DBE) level for this structure based on response spectrum for stiff soil conditions. The accelerogram scale factor for the DBE level was 1.275. The maximum roof displacement was measured as 3.0% of the building height, and the frame experienced inelastic deformation without significant strength degradation. After this test, the frame was straightened to eliminate the residual drift. Third, the structure was subjected to the Northridge Canoga Park (1994) ground motion record scaled to the maximum considered earthquake (MCE) level. The accelerogram scale factor for the MCE level was 1.912. The maximum roof displacement was measured as 3.7% of the building height. Plastic hinges formed in the beams, and a crack developed at the bottom of the first story middle column, resulting in a drop in shear capacity. Lastly, the frame was subjected to a second DBE, representing an aftershock. The maximum roof displacement was measured as 3.3% of the building height. The crack from the previous test propagated, and another crack was formed, but the frame did not collapse. Fig. 5(a) and (b) shows the computational and experimental displacement time-history results for the first and fourth floors corresponding to the design level (DBE), respectively, while Fig. 6(a) and (b), the same response quantities to the MCE loading. As can been seen from Figs. 5–6, the analysis results closely follow the experimental ones. Significant inelastic response was observed for both steel and CFT column members. However, the extent of damage was larger for the steel girders, which experienced yielding and local buckling under both design level and MCE.
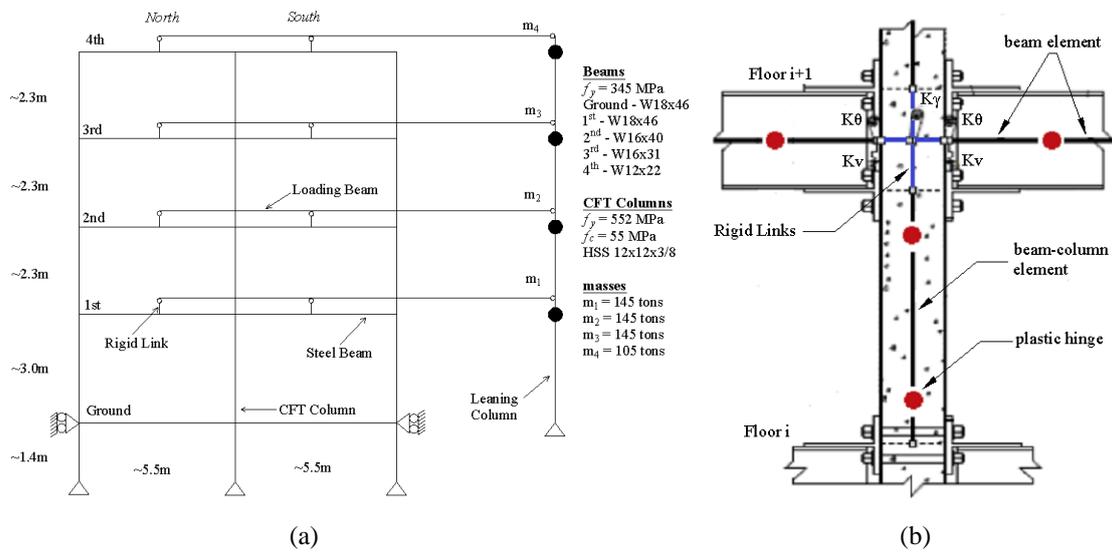
Fig. 4. (a) Test CFT-MRF by Herrera et al. [20] and (b) illustration of all models [35].
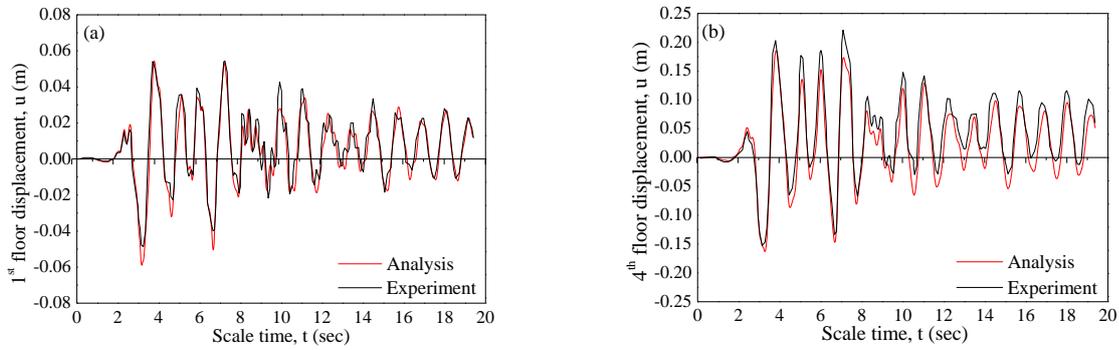
Fig. 5. Comparisons of experimental and computational results: (a) first-floor and (b) fourth-floor displacement history for DBE test [35].
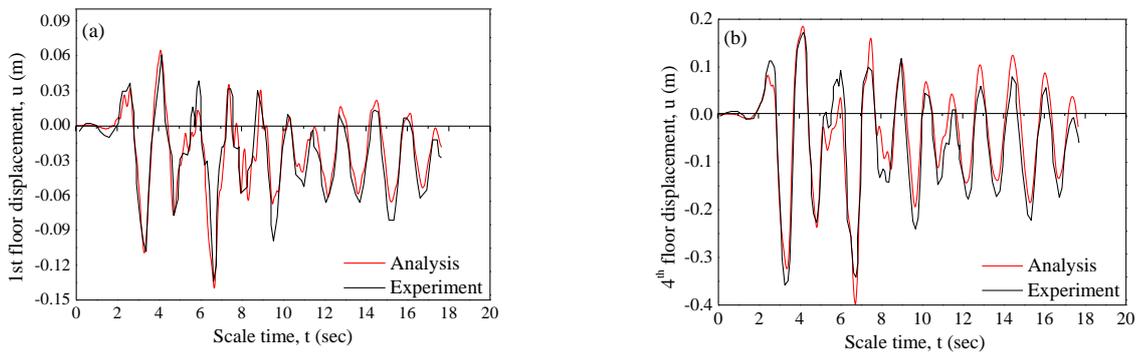
Fig. 6. Comparisons of experimental and computational results: (a) first-floor and (b) fourth-floor displacement history for MCE test [35].

4. Ground motions considered

A set of 100 ordinary (far-field type) ground motions recorded at soils with average shear wave velocity $v_{s,30}$ in the range between 360 and 800 m/s (classified according to Eurocode 8 [1] as soil type B) are selected from the PEER [37] database and are used for the nonlinear time history analyses of this study. Event magnitudes ranged from M 6.0 to M 7.5. The selection of these ordinary ground motions was made in such a way so that their geometric average spectrum is as close as possible to the Eurocode 8 [1] elastic spectrum for ground acceleration 0.30 g and soil type B. The acceleration response spectra of the selected 100 motions are shown in Fig. 7 against to the Eurocode 8 [1] elastic spectrum. A full list of all these ground motions with their characteristics can be found in Skalomenos [38].
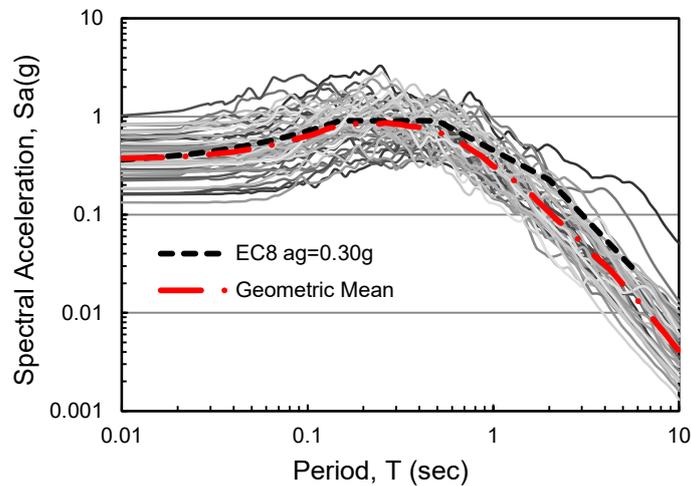

Fig. 7. Acceleration response spectra of the 100 earthquakes under consideration and comparison with Eurocode 8 [1] elastic spectrum.

5. Methodology for computation of damage expressions

In the present work, an extensive parametric study was conducted for the 48 CFT-MRFs of Table 1, which were subjected to the 100 ground motions of Fig. 7 for the evaluation of the damage expressions. The frames were analyzed with the program Ruaumoko 2D [23] using the incremental dynamic analysis method [39]. Thus, approximately 72000 analyses (=48 frames x 100 ground motions x 15 analyses on the average for every frame) were conducted in this work. These 15 on the average analyses for every frame correspond to 15 different PGA values for every ground motion.

The ground motion intensity level was measured here by an intensity measure equal to the spectral acceleration S_a, of the motion corresponding to the fundamental period of each frame. The structural response was measured by a damage measure equal to the maximum damage index

among all storeys that was recorded during the time history of the analysis. More specifically, each ground motion was continuously scaled by increasing its S_a until the frame to become dynamically unstable and collapse, while no limit of maximum drift was considered. The results of the analysis were post-processed in order to create a databank with the response quantities of interest.

The created databank is actually a spreadsheet with rows equal to the number of nonlinear analyses and columns equal to the response quantities of interest in columns and beams of a CFT-MRF along its height. Those response quantities are the maximum values of the following damage indices:1) Park and Ang damage index, D_{PA}, 2) Bracci et al. damage index, D_B, 3) Roufaiel and Meyer damage index, D_{RM} and 4) Banon and Veneziano damage index, D_{BV}. Moreover, the columns of the databank were increased by adding the characteristics of the frames (n_s, ρ, α) and the spectral acceleration S_a.

6. Damage formulae for moment resisting frames

In this section, simple formulae to estimate seismic damage, through four well known damage indices, of CFT-MRFs are proposed. Thus, with the aid of these simple expressions one can determine the maximum damage, D, of column bases or beams of this type of frames in terms of characteristics of the structure and the ground motions that excite them.

By analyzing the response databank, the proposed relationship was identified and thus the expression

$$D = b_1 \cdot n_s^{b_2} \cdot \alpha^{b_3} \cdot \left(\frac{S_a}{g} \right)^{b_4} \left(\frac{235}{f_s} \right)^{b_5} \tag{11}$$

with b_1, b_2, b_3, b_4 and b_5 constants to be determined, was selected as a good candidate for approximating the response databank. The aforementioned relation is relatively simple and satisfies the physical constraint $D=0$ for $S_a=0$. However, for nonzero values of S_a for which structural members behave elastically, Eq. (11) gives nonzero values of damage either at columns or beams, while in reality damage there is zero. Thus, before using this equation, one should compute the internal forces (bending moments M and axial forces P) of the columns or beams by performing a linear elastic analysis and check if their values are in the elastic range. This can be done by checking if the computed (M,P) combination lies inside the area enclosed by the M-P interaction diagram of Fig. 8 taken from the Ruaumoko computer program [23], where M0, PYT and PYC denote the yield moment at P = 0, the axial tension yield force and the axial compression yield force of a section, respectively. If the members are in the elastic range, the value of damage is equal to

zero by default, otherwise the proposed relationship can be used. Use of the Levenberg–Marquardt algorithm [30] for nonlinear regression analysis of the results of the parametric study, led to the following expressions for each one of the four damage indices
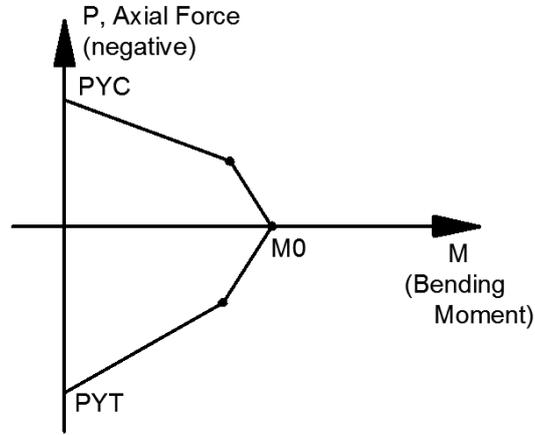

Fig. 8. M-P interaction diagram taken from the Ruaumoko computer program [23].

a) for column bases:

$$D_{PA}^{c} = 0.24 \cdot n_{s}^{0.16} \cdot \alpha^{-0.30} \cdot \left(\frac{S_{a}}{g} \right)^{0.39} \left(\frac{235}{f_{s}} \right)^{0.05} \tag{12}$$

$$D_{BRM}^{c} = 0.63 \cdot n_{s}^{0.12} \cdot \alpha^{-0.47} \cdot \left(\frac{S_{a}}{g} \right)^{0.26} \left(\frac{235}{f_{s}} \right)^{0.33} \tag{13}$$

$$D_{RM}^{c} = 0.45 \cdot n_{s}^{0.16} \cdot \alpha^{-0.46} \cdot \left(\frac{S_{a}}{g} \right)^{0.36} \left(\frac{235}{f_{s}} \right)^{0.45} \tag{14}$$

$$D_{BV}^{c} = 0.33 \cdot n_{s}^{0.12} \cdot \alpha^{-0.33} \cdot \left(\frac{S_{a}}{g} \right)^{0.39} \left(\frac{235}{f_{s}} \right)^{0.02} \tag{15}$$

b) for beams:

$$D_{PA}^{b} = 0.31 \cdot n_{s}^{0.33} \cdot \alpha^{-0.12} \cdot \left(\frac{S_{a}}{g} \right)^{0.43} \left(\frac{235}{f_{s}} \right)^{-0.08} \tag{16}$$

$$D_{BRM}^b = 0.49 \cdot n_s^{0.17} \cdot \alpha^{-0.08} \cdot \left(\frac{S_a}{g}\right)^{0.24} \left(\frac{235}{f_s}\right)^{-0.01} \tag{17}$$

$$D_{RM}^b = 0.28 \cdot n_s^{0.30} \cdot \alpha^{-0.17} \cdot \left(\frac{S_a}{g}\right)^{0.38} \left(\frac{235}{f_s}\right)^{-0.14} \tag{18}$$

$$D_{BV}^b = 0.40 \cdot n_s^{0.27} \cdot \alpha^{-0.06} \cdot \left(\frac{S_a}{g}\right)^{0.36} \left(\frac{235}{f_s}\right)^{-0.10} \tag{19}$$

With D being any damage index of interest, the mean, median and standard deviation of the ratio of the "exact" value of D obtained from inelastic dynamic analyses over the approximate one calculated from Eqs (12) to (19), respectively., i.e., D_{exact}/D_{app}, are used in order to express the central tendency and the dispersion of the error introduced by the proposed relations. Thus, these metrics for the damage indices used in this study are presented in Table 2. The values of those metrics show that the proposed formulae are fairly accurate. In addition, Fig. 9 depicts graphs of all the damage indices based on the proposed relationships versus their "exact" values for (a) columns and (b) beams.

Eqs (12) to (19) can also be utilized in the preliminary performance based design of structures in conjunction with elastic analysis in order to decrease the need for iterations in the analysis/design procedure. For this purpose, a flowchart showing how the design process should be conducted to take advantage of these equations is depicted in Fig. 10.

Table 2. Metrics of D_{exact}/D_{app} for all damage indices considered in this study.

D_{exact}/D_{app} (Column Bases)	Mean	Median	Standard Deviation
D_{PAM}	1.00	0.96	0.29
D_{BRM}	1.00	0.99	0.26
D_{RMO}	1.00	0.93	0.37
D_{BVM}	0.99	0.97	0.27
D_{exact}/D_{app} (Beams)	Mean	Median	Standard Deviation
D_{PAM}	0.99	0.96	0.27
D_{BRM}	1.00	0.98	0.18
D_{RMO}	1.00	0.98	0.27
D_{BVM}	0.99	0.98	0.23
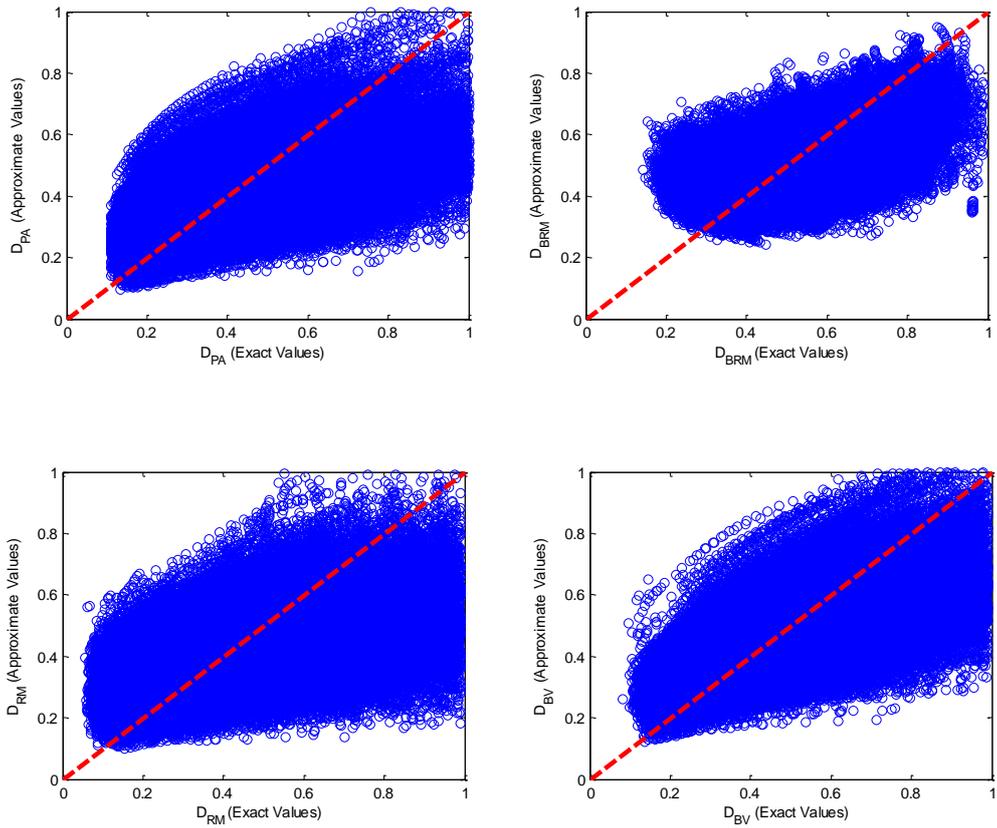
(a)
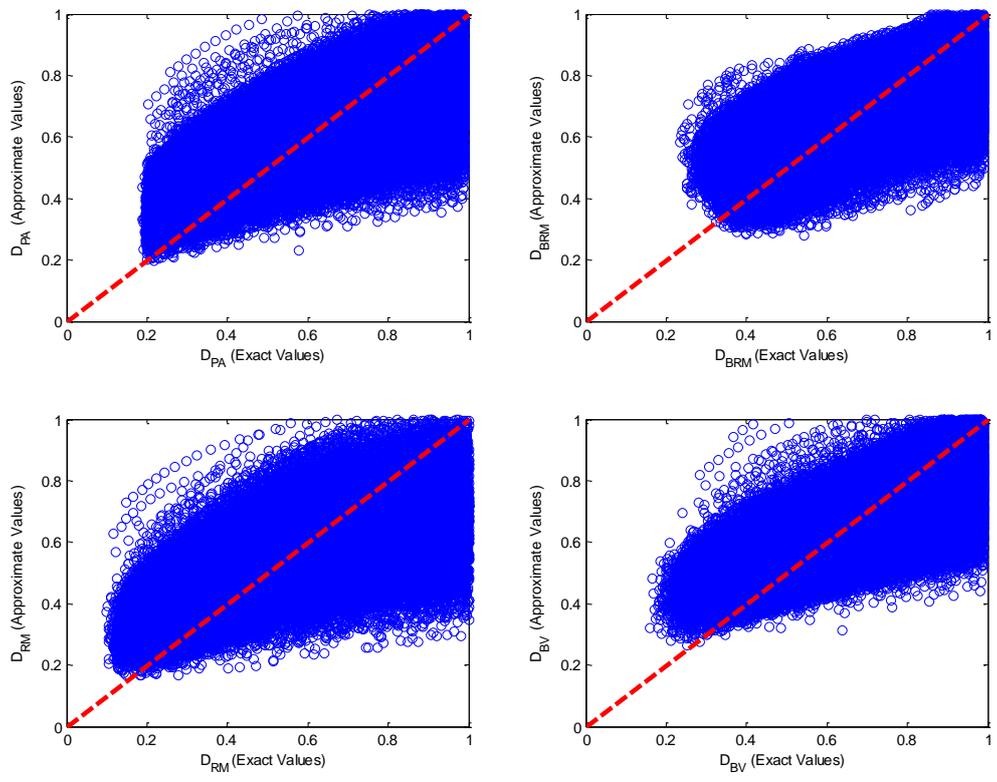
(b)

Fig. 9. Damage indices based on proposed equations versus exact values for (a) columns and (b) beams
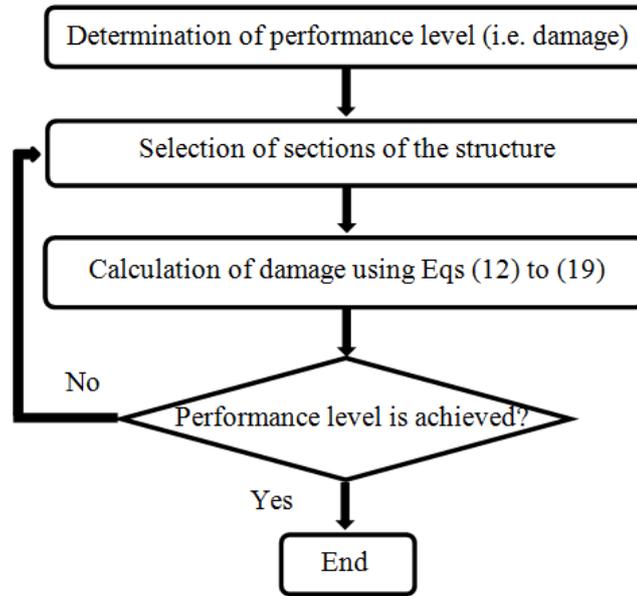
Fig. 10. Design process including proposed equations

7. Examples of application

In this section, three numerical examples are presented in order to illustrate the use of the proposed expressions and demonstrate their advantages and precision by comparing the results derived by them to the "exact" values of damage obtained by nonlinear dynamic analyses.

7.1 Three storey moment resisting frame

A three storey-three bay CFT-MRF is examined, with a geometrical configuration similar to the one shown in Fig. 2. The seismic load combination consists of the gravity load $G + 0.3Q = 27.5$ kN/m on beams plus the earthquake load and the gravity load combination $1.35G + 1.5 \cdot Q = 42.6$ kN/m. The frame has been designed in accordance with the provisions of structural Eurocodes, using design ground acceleration $\alpha_g = 0.30g$, soil type B (soil factor $S = 1.2$) and Spectrum Type 1 with behaviour factor $q = 4$. The yielding stress f_s takes the value of 275 MPa. The design yielded CFT columns with square steel tubes of width $b = 300$ mm and thickness $t = 12.5$ mm and IPE 240 beams for all the floors.

The characteristic value α of the frame was computed on the basis of Equation (10) and found to be equal to 2.322. The expected ground motion was defined by the acceleration response spectrum of EC8 [1] with a PGA equal to 0.35 g and a soil of class B. The fundamental period of vibration, T, of the frame is equal to 0.844 s, while its spectral acceleration S_a corresponding to this period, derived in the basis of EC8 [1] spectrum, equals 0.64 g.

Eight semi-artificial accelerograms compatible with the EC8 [1] spectrum were generated via a deterministic approach [40] on the basis of the eight real seismic records of Table 3. The response

spectra of these motions, in comparison with the EC8 [1] spectrum, are depicted in Fig. 11. Nonlinear time history analyses of the designed frame under these motions were performed. The four damage indices used here and observed in column bases and beams of the frame were computed with the aid of the program Ruaumoko 2D [23]. Then, the mean value of the maximum damage values for the eight semi-artificial accelerograms was evaluated for each damage index. Before using the proposed formulae, the internal forces (bending moments M and axial forces P) of the columns or beams were computed by performing a linear elastic analysis and it was checked if their values are in the elastic range as explained in Section 6. It was found that both the column bases and beams were not in the elastic range. Thus, the approximate values of the damage indices were computed with the aid of Eqs (12)-(19) and recorded together with the exact ones in Tables 4 and 5 for column bases and beams, respectively. The proposed relations predict satisfactorily the damage of the beams (error = 5.6-9.5%) for all kinds of indices. For the columns bases damage is also predicted fairly well (error = 4.7-16.0%) for all kinds of indices. Thus, the predictions of the proposed formulae are quite close to the "exact" ones and as far as the columns are concerned, in most of the cases, on the safe (conservative) side as being larger than the "exact" ones.

Table 3. Characteristics of ground motions used in the examples.

| No.	Date	Record Name	Comp.	Station Name	PGA (g)
1.	1992/04/25	Cape Mendocino	NS	89509 Eureka	0.154
2.	1992/06/28	Landers	N045	24577 Fort Irwin	0.114
3.	1994/01/17	Northridge	EW	24389 LA - Century City CC North	0.256
4.	1994/01/17	Northridge	EW	24538 Santa Monica City Hall	0.883
5.	1994/01/17	Northridge	EW	24400 LA - Obregon Park	0.355
6.	1994/01/17	Northridge	EW	127 Lake Hughes #9	0.165
7.	1994/01/17	Northridge	N035	90014 Beverly Hills- 12520 Mulhol	0.617
8.	1994/01/17	Northridge	EW	24401 San Marino, SW Academy	0.116
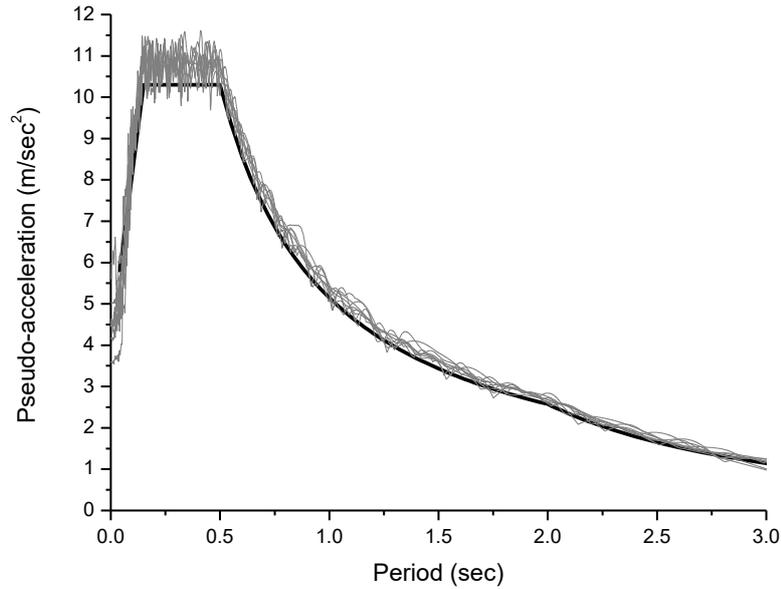
Fig. 11. Response spectra of ground motions used in the examples of Section 7.

Table 4. Comparison between "exact" and approximate values of damage indices for columns of the CFT-MRF of the example of Section 7.1.

Damage Index	"Exact" Value	Approximate Value	Error(%)
D_{PAM}	0.157	0.187	16.0
D_{BRM}	0.436	0.411	5.6
D_{RMO}	0.273	0.287	4.7
D_{BVM}	0.203	0.240	15.7

Table 5. Comparison between "exact" and approximate values of damage indices for beams of the CFT-MRF of the example of Section 7.1.

Damage Index	"Exact" Value	Approximate Value	Error(%)
D_{PAM}	0.355	0.335	5.6
D_{BRM}	0.544	0.500	8.1
D_{RMO}	0.315	0.295	6.4
D_{BVM}	0.494	0.447	9.5

7.2 Six storey moment resisting frame

A six storey-three bay CFT-MRF is examined, with a geometrical configuration similar to that shown in Fig. 2. The seismic load combination consists of the gravity load G + 0.3Q = 27.5 kN/m on beams plus the earthquake load and the gravity load combination 1.35G + 1.5·Q = 42.6 kN/m. The frame has been designed in accordance with the provisions of structural Eurocodes, using design ground acceleration α_g = 0.30g, soil type B (soil factor S = 1.2) and Spectrum Type 1 with behaviour factor q = 4. The yielding stress f_s takes the value of 275 MPa.

20

The characteristic value α of the frame was computed on the basis of Equation (10) and found to be equal to 3.17. The fundamental period of vibration, T, of the frame and the corresponding spectral acceleration S_a from the EC8 [1] spectrum were equal to equal to 1.204 s and 0.45 g, respectively.

The records of the previous example are again used here. Nonlinear time history analyses of the designed frame under these motions were performed. The four damage indices used here and observed in column bases and beams of the frame were computed with the aid of the program Ruaumoko 2D [23]. Then, the mean value of the maximum damage values for the eight semi-artificial accelerograms was calculated for each damage index. Before using the proposed formulae, the internal forces (bending moments M and axial forces P) of the columns or beams were computed by performing a linear elastic analysis and it was checked if their values are in the elastic range as explained in Section 6. It was found that only the column bases were in the elastic range. Thus, the values of the damage indices at the column bases were set equal to zero by default and Eqs (12)-(15) were not used in this case. Moreover, the approximate values of the damage indices for the beams were computed with the aid of Eqs (16)-(19) and recorded together with the exact ones in Table 6. The proposed relations predict the damage of the beams with high accuracy (error = 6.8 - 8.8%) for all kinds of indices, and they are on the safe (conservative) side, in most of the cases.

Table 6. Comparison between "exact" and approximate values of damage indices for beams of the CFT-MRF of the example of Section 7.2.

Damage Index	"Exact" Value	Approximate Value	Error(%)
D_{PAM}	0.321	0.346	7.2
D_{BRM}	0.466	0.500	6.8
D_{RMO}	0.279	0.300	7.0
D_{BVM}	0.509	0.464	8.8

7.3 Composite MRF of Herrera et al. [20]

The composite MRF investigated experimentally by Herrera et al. [20] is used herein as an example for the validation of the proposed relationships. The characteristics of the frame and all its design details are given in subsection 3.3 and are different than that used for the parametric studies. This is done to test the proposed equations for a frame configuration different than that used for the calibration of the proposed equations.

The characteristic value α of the frame was computed on the basis of Equation (10) and found to be equal to 1.087. The expected ground motion was defined by the acceleration response spectrum of EC8 [1] with a PGA equal to 0.35 g and a soil of class B. The fundamental period of vibration,

T, of the frame is equal to 1.108 s, while its spectral acceleration S_a corresponding to this period, derived in the basis of EC8 [1] spectrum, equals 0.49 g.

The records of the example in subsection 7.1 are again used here. Nonlinear time history analyses of the designed frame under these motions were performed. The four damage indices used here and observed in column bases and beams of the frame were computed with the aid of the program Ruaumoko 2D [23]. Then, the mean value of the maximum damage values for the eight semi-artificial accelerograms was calculated for each damage index. Before using the proposed formulae, the internal forces (bending moments M and axial forces P) of the columns or beams were computed by performing a linear elastic analysis and it was checked if their values are in the elastic range as explained in Section 6. It was found that only the column bases were in the elastic range. Thus, the values of the damage indices at the column bases were set equal to zero by default and Eqs (12)-(15) were not used in this case. Moreover, the approximate values of the damage indices for the beams were computed with the aid of Eqs (16)-(19) and recorded together with the exact ones in Table 7. The proposed relations predict the damage of the beams fairly well (error = 11.7 - 20.5%) for all kinds of indices, and they are on the safe (conservative) side, for the cases of Bracci et al. [10] and Roufaiel and Meyer [6] damage indices. The prediction of the damage indices of this example was not as accurate as that of the previous examples. This is logical, because the frame used here has different structural characteristics (e.g. storey height and bay width) than the frames used in the parametric studies. However, this prediction can be considered as satisfactory, since it was managed to estimate damage of a frame with different structural configuration and properties than those used for the derivation of the proposed equations.

Table 7. Comparison between "exact" and approximate values of damage indices for beams of the CFT-MRF of the example of Section 7.3.

Damage Index	"Exact" Value	Approximate Value	Error(%)
D_{PAM}	0.462	0.408	11.7
D_{BRM}	0.432	0.512	15.6
D_{RMO}	0.389	0.448	13.2
D_{BVM}	0.658	0.523	20.5

8. Conclusions

A procedure in terms of simple formulae for estimating the maximum damage in regular multi-storey CFT-MRFs subjected to ordinary (i.e. without near-fault pulses effects) ground motions has been presented. Particularly, simple and easy to use relationships were derived for the computation of four damage indices of the literature, which take into account the influence of basic characteristics of CFT-MRFs and ground motions, such as the number of stories, beam strength

ratio, steel yielding stress ratio and spectral acceleration. The scope of the frames used in this study is to represent the behaviour of a wide range of CFT-MRFs, including structures from low to high number of storeys, which can be implemented in common practice. It should be noticed herein that the proposed relations are valid for frames with characteristics similar to those of the frames used in the parametric study and for seismic sites where ordinary ground motions are expected. These expressions give a good approximation of damage and provide a rapid damage assessment of existing structures without the use of the more sophisticated and time consuming non-linear dynamic analysis. Finally, They can also be utilized in the preliminary design of structures in conjunction with elastic analysis in order to decrease the need for iterations in the analysis/design procedure.

References

[1]   EC8. Design of structures for earthquake resistance, Part 1: General rules, seismic actions and rules for buildings, European Committee for Standardization (CEN), Brussels, Belgium, 2004.

[2]   Fajfar P and Krawinkler H. Seismic Design Methodologies for the Next Generation of Codes. Bled, 24-27 June 1997, Balkema, Rotterdam.

[3]   FEMA. FEMA-273 Building Seismic Safety Council, NEHRP guidelines for the seismic rehabilitation of buildings. Federal Emergency Management Agency, Washington (DC), 1997.

[4]   Kamaris GS, Hatzigeorgiou GD, Beskos DE. Direct damage controlled seismic design of plane steel degrading frames. Bulletin of Earthquake Engineering, 2015; 13(2):587-612.

[5]   Banon H, Veneziano D. Seismic safety of reinforced concrete members and structures. Earthquake Engineering and Structural Dynamics 1982; 10:179-173.

[6]   Roufaiel MS, Meyer C. Analytical modeling of hysteretic behavior of R/C frames. Journal of Structural Engineering, ASCE 1987; 113:429-444.

[7]   Cosenza E, Manfredi G, Ramasco R. The use of damage functionals in earthquake engineering: A comparison between different methods. Earthquake Engineering and Structural Dynamics 1993; 22(10):855-868.

[8]   Stephens JE, Yao JTP. Damage assessment using response measurements. Journal of Structural Engineering, ASCE 1987; 113:787-801.

[9]   McCabe SL, Hall WJ. Assessment of seismic structural damage. Journal of Structural Engineering, ASCE 1989; 115: 2166-2183.

[10] Bracci JM, Reinhorn, AM, Mander JB. Deterministic model for seismic damage evaluation of reinforced concrete structures, Technical Report NCEER 89-0033, State University of New York at Buffalo, 1989.

[11] Krawinkler H, Zohrei M. Cumulative damage in steel structures subjected to earthquake ground motions. Computers and Structures 1983; 16:531-541.

[12] Sucuoğlu H, Erberik A. Energy-based hysteresis and damage models for deteriorating systems. Earthquake Engineering and Structural Dynamics 2004; 33: 69-88.

24

[13] Kamaris GS, Hatzigeorgiou GD, Beskos DE. A new damage index for plane steel frames exhibiting strength and stiffness degradation under seismic motion. Engineering Structures, 2013; 46:727-736.

[14] Park Y-J, Ang AH-S. Mechanistic seismic damage model for reinforced concrete. Journal of Structural Engineering, ASCE 1985; 111:722-739.

[15] Powell GH, Allahabadi R. Seismic damage prediction by deterministic methods: concepts and procedures. Earthquake Engineering and Structural Dynamics 1988; 16: 719-734.

[16] Lemaitre J. A Course on Damage Mechanics. Springer-Verlag, Berlin, 1992.

[17] Hatzigeorgiou GD, Beskos DE. Direct damage controlled design of concrete structures. Journal of Structural Engineering, ASCE 2007; 133:205-215.

[18] Kamaris GS, Hatzigeorgiou GD, Beskos DE. Direct damage controlled design of plane steel-moment resisting frames using static inelastic analysis. Journal of Mechanics of Materials and Structures 2009; 4:1375-1393.

[19] Hajjar JF. Composite steel and concrete structural systems for seismic engineering. J Constr Steel Res 2002; 58: 703-728.

[20] Herrera RA, Ricles JM, Sause R.Seismic Performance Evaluation of a Large-Scale Composite MRF Using Pseudodynamic Testing. J Struct Eng ASCE 2008; 134(2): 279-288.

[21] Skalomenos, K.A., Hatzigeorgiou, G.D., Beskos, D.E. Seismic behavior of composite steel/concrete MRFs: Deformation assessment and behavior factors", Bulletin of Earthquake Engineering 2015; Online first.

[22] Kamaris GS, Vallianatou Y-M, Beskos DE. Seismic damage estimation of in-plane regular steel moment resisting and x-braced frames. Bulletin of Earthquake Engineering 2012; 10(6):1745-1766.

[23] Carr AJ. Ruaumoko-2D. Inelastic Time-History Analysis of Two-Dimensional Framed Structures, Department of Civil Engineering. University of Canterbury, New Zealand, 2006.

[24] Castiglioni CA, Pucinotti R. Failure criteria and cumulative damage models for steel components under cyclic loading. Journal of Constructional Steel Research 2009; 65:751-765.

[25] Du X-K, Wang T-C, He H, Yi K. Experimental Research and Damage Model of Square Concrete-Filled Steel Tube Subjected to Cyclic Loading. ICCTP 2009 : Critical Issues in Transportation Systems Planning, Development, and Management, ASCE, 2009.

[26] EC4: Design of composite steel and concrete structures - Part 1.1: General rules and rules for buildings, European Committee for Standardization (CEN), Brussels, Belgium, 2004.

[27] Karavasilis TL, Bazeos N, Beskos DE. Drift and Ductility Estimates in Regular Steel MRF Subjected to Ordinary Ground Motions: A Design-Oriented Approach. Earthquake Spectra 2008; 24(2):431-451.

[28] EC3. Design of steel structures - Part 1.1: General rules and rules for buildings, European Committee for Standardization (CEN), Brussels, Belgium, 2005.

[29] SAP2000. Static and Dynamic Finite Element Analysis of Structures - V16. Computers and Structures Inc., Berkeley, California, 2013.

[30] MATLAB. The language of technical computing, Version 5.0. The Mathworks Inc., Natick, Mass, 2009.

[31] Castro, J.M., Elghazouli, A.Y., Izzuddin, B.A. Modeling of the panel zone in steel and composite moment frames. Engineering Structures 2005; 27:129–144.

[32] Skalomenos KA, Hatzigeorgiou GD, Beskos DE. Parameter identification of three hysteretic models for the simulation of the response of CFT columns to cyclic loading. Engineering Structures 2014; 61:44-60.

[33] Lignos DG, Krawinkler HK. Deterioration modeling of steel components in support of collapse prediction of steel moment frames under earthquake loading. Journal of Structural Engineering, ASCE, 2011; 137(11): 1291-1302.

[34] PEER/ATC. Modeling and Acceptance Criteria for Seismic Analysis and Design of Tall Buildings. Report No 72-1, Applied Technology Council. Redwood City, California, 2010.

[35] Skalomenos KA, Hatzigeorgiou GD, Beskos DE. Modelling level selection for seismic analysis of CFT/MRFs by using fragility curves. Earthquake Engineering Structural Dynamics 2015; 44(2): 199-220.

[36] Zhao XL, Han LH, Lu H. Concrete-filled Tubular Members and Connections. Spon Press, New York, 2010.

[37] NGA Strong ground motion database. Pacific Earthquake Engineering Research Center, /http://peer.berkeley.edu, 2011.

[38] Skalomenos KA. Seismic performance of plane moment resisting frames with concrete filled steel tube columns and steel I beams. Ph.D. Dissertation, Department of Civil Engineering, University of Patras, Greece, 2014, http://hdl.handle.net/10889/8442.

[39] Vamvatsikos D. Cornell CA. Incremental dynamic analysis. Earthquake Engineering Structural Dynamics 2002; 31(3):491-514.

[40] Karabalis DL, Cokkinides GJ, Rizos DC. Seismic Record Processing Program-Ver.1.03, Report of the College of Engineering, University of South Carolina, Columbia, 1992.